

# Practical specification of the speech universe of the maximum power point tracking controller based on the asymmetrical fuzzy logic: a dynamic behavior study of the photovoltaic system

Ahmed Amine Barakate, Sami Choubane, Abdelkader Hadjoudja

Laboratory of Electronic Systems, Information Processing and Energetics, Ibn Tofail University, Kenitra, Morocco

## Article Info

### Article history:

Received Aug 7, 2024

Revised Apr 2, 2025

Accepted Jul 12, 2025

### Keywords:

Asymmetrical fuzzy logic controller

Efficiency of photovoltaic

Fuzzy logic controller

Maximum power point tracker

Stand-alone photovoltaic system

## ABSTRACT

In this paper, we present a procedure for extracting data from a stand-alone photovoltaic (PV) panel to program a maximum power point tracking (MPPT) controller based on the fuzzy logic (FL) method, aiming to optimize the performance of the photovoltaic system. Photovoltaic data acquisition enables the determination of the input and output speech universe for the MPPT controller using fuzzy logic. This method adapts to nonlinear systems without requiring a complex mathematical model. Additionally, it improves the performance of the photovoltaic system in both dynamic and steady-state conditions. To further enhance the method's efficiency, an asymmetric membership function concept is proposed based on the dynamic behavior study of the photovoltaic system. Compared to the symmetric method, the asymmetric fuzzy logic controller achieves higher maximum power output and better tracking precision. This technology is essential for maximizing photovoltaic panel efficiency, a key requirement as solar energy gains prominence as a clean and renewable energy source.

*This is an open access article under the [CC BY-SA](https://creativecommons.org/licenses/by-sa/4.0/) license.*



## Corresponding Author:

Ahmed Amine Barakate

Laboratory of Electronic Systems, Information Processing and Energetics, Ibn Tofail University Kenitra

Kenitra, Morocco

Email: [ahmedamine.barakate1@uit.ac.ma](mailto:ahmedamine.barakate1@uit.ac.ma)

## 1. INTRODUCTION

In recent years, concerns over greenhouse gas emissions and escalating fuel prices have intensified the demand for alternative energy sources. Among these, solar energy is one of the most sustainable and inexhaustible resources. However, due to the nonlinear variation of current (I) and voltage (V) characteristics of photovoltaic (PV) cells under different irradiation and temperature conditions, it is crucial to operate PV systems at specific points to extract maximum solar energy. This process, known as maximum power point tracking (MPPT), ensures efficient energy utilization. Various MPPT methods have been developed and implemented in previous studies [1]–[3], including perturbation and observation (P&O), incremental conductance, fractional open circuit voltage, fractional short circuit current, and fuzzy logic (FL) techniques. These methods offer high tracking accuracy but often face trade-offs between tracking speed and precision under varying insolation conditions.

Fuzzy logic is advantageous as it does not require a precise and complicated mathematical model and can handle highly nonlinear systems. Consequently, MPPT algorithms based on FL have attracted significant research interest [4]–[7]. Recently, many MPPT techniques based on FL have been proposed in the literature. Compared to conventional algorithms, FL-based MPPT techniques demonstrate improved tracking performance, response time and power efficiency under fluctuating climatic conditions, such as

temperature variations and shading. However, the design considerations and the complexity of implementing FL-based MPPT techniques vary significantly, necessitating further investigation into their optimization.

**2. PROPOSED PHOTOVOLTAIC SYSTEM**

The proposed system, illustrated in Figure 1, offers an innovative solution for generating stable power from a photovoltaic panel. It comprises a PV panel, a DC/DC static energy conversion unit [8]–[10], a load, and a block for calculating the maximum power point (MPP), which controls the converter. The DC/DC converter serves as an interface between the PV panels and the storage system [11], [12], regulating voltage and current to maintain a stable and optimal power output regardless of temperature and solar irradiance variations. To ensure real-time maximum power generation, an intelligent MPPT system based on fuzzy logic enables the converter to adapt the panel’s power output to match the load’s requirements [13]–[16]. The MPPT algorithm determines the optimal duty cycle for the converter based on input parameters, ensuring efficient and stable power generation. The maximum power output of a photovoltaic generator is heavily influenced by climatic conditions, with MPP varying proportionally with irradiation (G) and inversely with temperature (T).

The creation of the inference table plays a key role in controlling the fuzzy logic technique. There are two types of inference tables: the first, presented in Table 1, is a symmetrical fuzzy logic controller (FLC) derived from the power curve as a function of PV voltage in Figure 2. The second type is asymmetrical, based on an analysis of the photovoltaic panel's behavior under varying climatic conditions [17], [18].

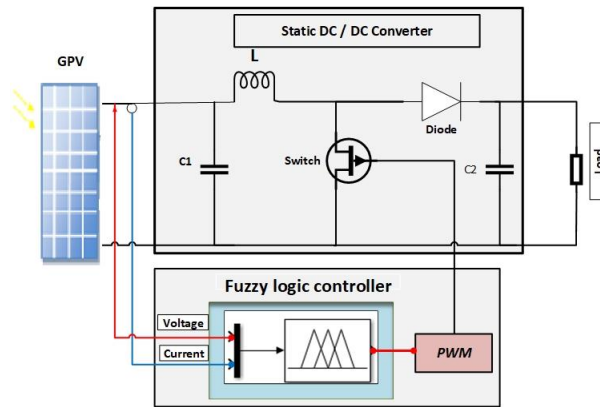


Figure 1. System block diagram

Table 1. Inference table for symmetrical FLC

	CE	NB	Ns	ZE	PS	PB
E						
NB	ZE	ZE	NG	NG	NG	
NS	ZE	ZE	NP	NP	NP	
ZE	NP	ZE	ZE	ZE	PP	
PS	PP	PP	PP	ZE	ZE	
PB	PG	PG	PG	ZE	ZE	

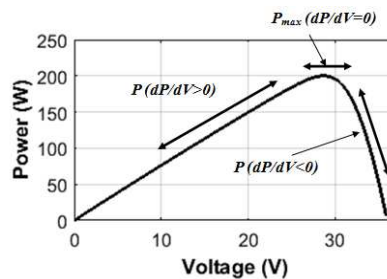


Figure 2. P-V curve of a solar panel

**3. BEHAVIORAL STUDY AND CONFIGURATION**

**3.1. Characterization of the API156P200 photovoltaic panel**

**3.1.1. Technical characteristics of the photovoltaic panel**

We simulated our API156P200 type photovoltaic panel with a static load of  $R_S=60 \Omega$  at the output. The panel's modularity and lightweight design make it well-suited for remote applications, including water pumping systems, domestic installations, and military use [19]. Additionally, the API156P200 panels can be easily connected in series or parallel configurations to meet varying energy demands. The technical specifications of the API156P200 PV panel are presented in Table 2.

Table 2. Technical characteristics of PV API156P200

Technical data	ABBR	Unit	Value
Maximum power for STC	$P_{max}$	W	$200 \pm 3\%$
Voltage at maximum power point	$V_{mpp}$	V	28.7
Current at maximum power point	$I_{mpp}$	A	6.97
Short circuit current	$I_{sc}$	A	7.75
Open circuit voltage	$V_{oc}$	V	36
Series resistance	$R_S$	$\Omega$	0.41727
Shent resistance	$R_{SH}$	$\Omega$	71.1705
Number of cells in series	$N_S$	-	60
Number of cells in parallel	$N_P$	-	01
Diode ideality factor	n	-	0.9655

**3.1.2. Electrical study of the photovoltaic panel**

The maximum power output of a GPV photovoltaic generator is significantly influenced by variations in irradiance and temperature. As shown in Figure 3, the photovoltaic panel responds to changes in these factors, demonstrating that power output and the maximum power point (MPP) vary proportionally with irradiance Figure 3(a) and temperature Figure 3(b) [20], [21]. Table 3 summarizes the calculated results of the electrical quantities of the photovoltaic panel. By determining the maximum power at a given temperature and irradiance, we establish that each maximum power corresponds to a specific duty cycle D, derived from (1), which allows us to determine the inference rules of the fuzzy logic control.

$$D = 1 - \sqrt{\frac{R_0}{R_s}} \quad \text{with} \quad R_0 = \frac{V_{ppm}^2}{P_{max}} \tag{1}$$

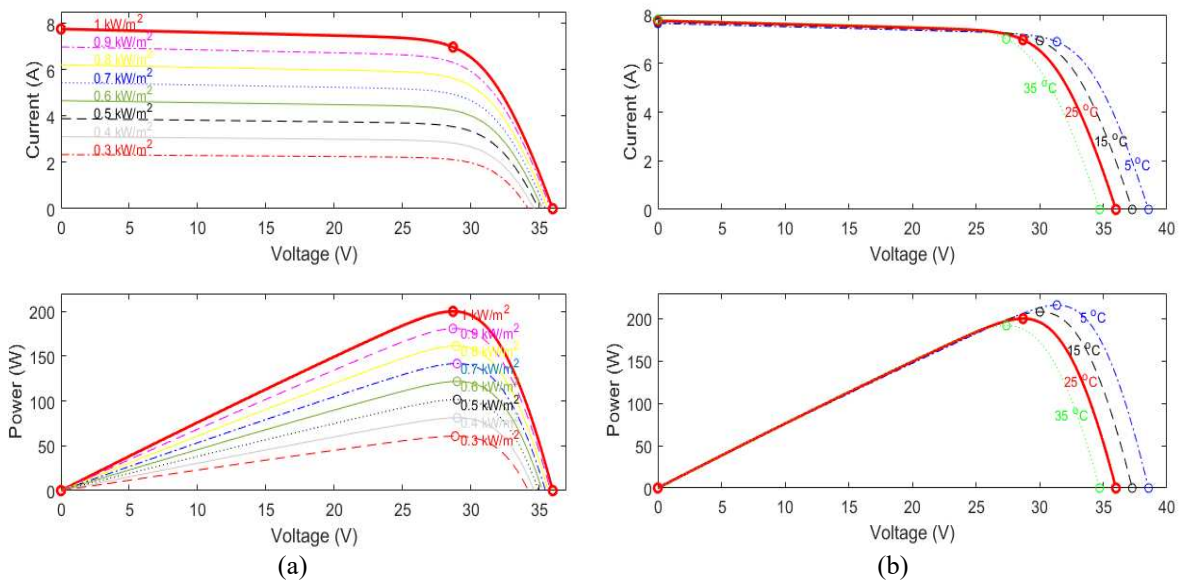


Figure 3. Power and current characteristics of PV as a function of voltage (a) at  $T=25 \text{ }^\circ\text{C}$  and various G and (b) at  $G=1000 \text{ W/m}^2$  and various T

Table 3. Maximum PV powers and their duty cycles

T (°C)	G (W/m <sup>2</sup> )	P <sub>max</sub> (W)	I <sub>ppm</sub> (A)	V <sub>ppm</sub> (V)	R <sub>0</sub> (Ω)	D
35	1000	191.8	7.00255568	27.39	3.91142909	0.74467573
25	1000	200	6.96864111	28.7	4.11845	0.7380
15	1000	208.1	6.9320453	30.02	4.33061221	0.73134247
5	1000	216	6.8877551	31.36	4.55300741	0.72453048
25	900	180.9	6.30533287	28.69	4.55011664	0.725
25	800	161.5	5.58437068	28.92	5.17873932	0.706
25	700	141.8	4.89134184	28.99	5.92679901	0.68571
25	600	121.9	4.20489824	28.99	6.89434044	0.661
25	500	101.7	3.50810624	28.99	8.2637178	0.6289
25	400	81.3	2.80344828	29	10.3444034	0.5848
25	300	60.74	2.1046431	28.86	13.7125387	0.5219

### 3.2. Configuration of the fuzzy logic MPPT command

In this section, we present the steps involved in configuring the fuzzy logic control. First, we present the calculator diagram, followed by an explanation of the data extraction process from the photovoltaic panel. This process is used to generate the input table (slope and its variation) and, subsequently, the inference table [22].

#### 3.2.1. Calculator diagram

The fuzzy Logic control system consists of a calculator for the slope ( $E$ ) and its variation ( $CE$ ), derived from (2) and (3), along with a fuzzy logic controller block. The schematic of the proposed control system is presented in Figure 4. It shows the computation flow of the slope and its variation based on the photovoltaic voltage  $V_{PV}$  and the current  $I_{PV}$  of the PV.

$$E = \frac{P(k) - P(k-1)}{V(k) - V(k-1)} \tag{2}$$

$$CE = E(k) - E(k - 1) \tag{3}$$

Based on the values of  $E$  and  $CE$  received by the LF controller (fuzzy logic block), the latter determines the value of the duty cycle  $D$  to control the converter. The PWM block, pulse width modulation, is implemented to generate a logic signal with a fixed frequency, while its duty cycle is digitally controlled. The average output signal corresponds to the duty cycle.

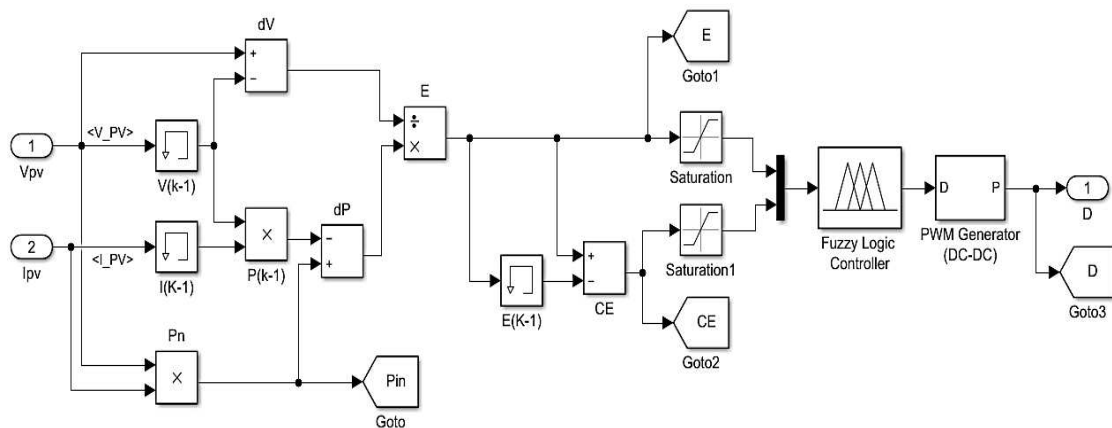


Figure 4. Calculator diagram MPPT

#### 3.2.2. Acquiring PV data to configure fuzzy logic control

In order to configure the fuzzy logic MPPT controller, we carried out a study about the dynamic behavior of the photovoltaic panel under varying climate conditions. In each scenario, we fixed the values of illumination and temperature, then recorded the corresponding slope  $E$  and its variation  $CE$ . This process allowed us to create a comparative table of the data and to define the table of inference rules. To perform this

step of extracting data  $E$  and  $CE$  from the photovoltaic panel, it is necessary to maintain the inputs (temperature and irradiation) and their corresponding duty cycle  $D$  fixed in Figure 5. The values of the slope and its variation are then recorded in registers for subsequent data extraction.

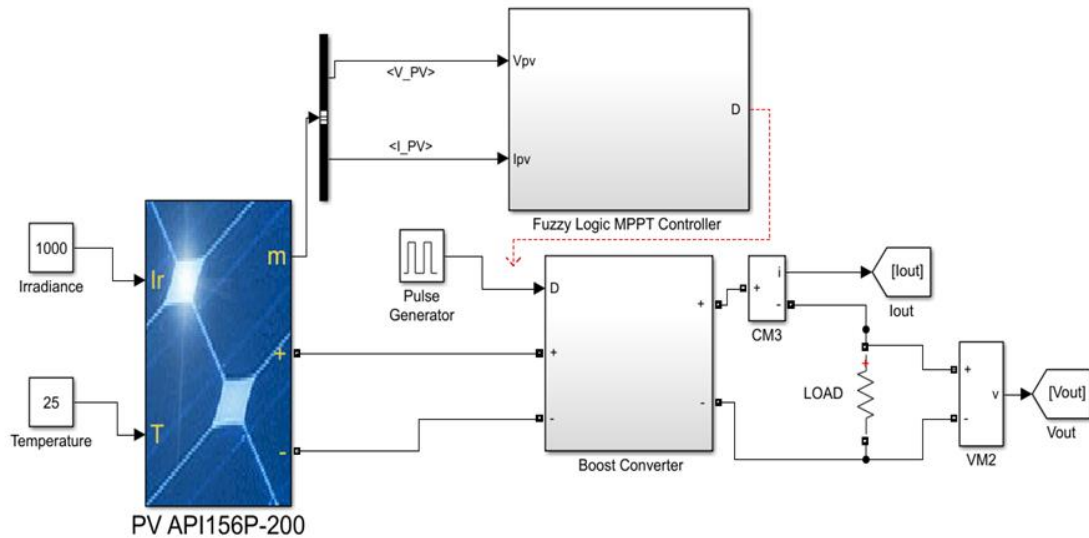


Figure 5. Photovoltaic system controlled by pulse generator

To set the duty cycle ( $D$ ), we replaced the output of the MPPT controller with a pulse generator that generates an appropriate command signal based on the proposed temperature and irradiance conditions, as outlined in Table 3. The data analyzed constitutes a sample because the number of recorded data is very large. The data acquired from the registers at irradiance levels of 1,000, 800, 600 and 400  $W/m^2$  at a temperature set at 25  $^{\circ}C$ , are categorized based on the sign of the variation in the slope  $CE$  and then sorted by slope  $E$ . These data are presented side-by-side in Tables 4 and 5 to define the ranges of the input variables used in the membership functions for the fuzzification step.

Table 4. Data ( $E$  and  $CE$ ) for variations of the positive slope at  $T=25^{\circ}C$

Slope E G=1000	Variation of slope CE	Slope E G=800	Variation of slope CE	Slope E G=600	Variation of slope CE	Slope E G=400	Variation of slope CE
8.70	-0.00042101						
8.50	-0.00167844						
8.00	-1.04E-05						
7.50	-0.00014833						
7.00	-0.0003222						
6.50	-0.00036789	6.09	-0.00052272				
6.00	-0.00066376	6.00	-0.00123774				
5.50	-0.00100111	5.50	-3.43E-05				
5.00	-0.00128443	5.00	-0.00024329				
4.50	-0.00156775	4.50	-0.00062369	4.20	-0.00061499		
4.00	-0.00213824	4.00	-0.00114381	4.00	-4.79E-06		
3.50	-0.00267634	3.50	-0.00040338	3.50	-0.00030515	3.49	-3.17E-05
3.00	-0.00331888	3.00	-0.00297618	3.00	-0.00067263	3.00	-0.00011826
2.50	-0.00332406	2.50	-0.00449437	2.50	-0.0012558	2.50	-0.00085923
2.00	-0.00486649	2.00	-0.00341651	2.00	-0.00291598	2.00	-0.00097606
1.60	-0.00645323	1.60	-0.00208857	1.60	-0.00132035	1.60	-0.00378054
1.20	-0.00908187	1.20	-0.02251827	1.20	-0.00170439	1.20	-0.0154896
1.00	-0.01036372	1.00	-0.02086137	1.00	-0.00271238	1.00	-0.02382885
0.80	-0.01149589	0.80	-0.02612243	0.80	-0.0028135	0.80	-0.00421297
0.60	-0.01351177	0.61	-0.00437407	0.60	-0.0012474	0.60	-0.00237943
0.41	-0.00472383	0.40	-0.00343077	0.40	-0.03969718	0.40	-0.00357554
0.20	-0.0170821	0.20	-0.01695149	0.20	-0.0394607	0.20	-0.03129312
0.01	-0.01090465	0.01	-0.00816985	0.01	-0.00165329	0.01	-0.00457984

Table 5. Data (E and CE) for variations in the negative slope at T=25 °C

Slope E G=1000	Variation of slope CE	Slope E G=800	Variation of slope CE	Slope E G=600	Variation of slope CE	Slope E G=400	Variation of slope CE
6.00	0.00062998						
5.50	0.00066269						
5.00	0.00096514	5.00	0.00013253				
4.50	0.00204884	4.50	0.0006217				
4.00	0.00244095	4.00	0.00061686				
3.50	0.00226211	3.50	0.00074249	3.50	0.00018663		
3.00	0.00394684	3.00	0.00535207	3.00	0.00096842	3.00	7.05E-05
2.50	0.00833822	2.50	0.00774603	2.50	0.00046327	2.50	0.000503044
2.00	0.00388685	2.00	0.00524147	2.00	0.00180262	2.00	0.002061292
1.60	0.00599562	1.60	0.03395077	1.60	0.00366051	1.60	0.000767493
1.20	0.00715978	1.20	0.00083586	1.20	0.0158861	1.20	0.006526618
1.00	0.01859265	1.00	0.00899469	1.00	0.02206532	1.00	0.004152771
0.80	0.0024678	0.80	0.03442196	0.80	0.02039325	0.80	0.005378488
0.60	0.00278337	0.60	0.02104486	0.60	0.00028167	0.60	0.001092519
0.40	0.01537842	0.40	0.00261814	0.40	0.01282358	0.40	0.031532075
0.21	0.00107194	0.21	0.00732076	0.20	0.00899597	0.20	0.039772257
0.01	0.00116542	0.01	0.00541131	0.01	0.00113619	0.01	0.002230987

**3.3. Fuzzification**

Fuzzification is a preliminary step that determines the subsets or intervals of maximum variation allowed in the input variables. The purpose of fuzzification is to convert the input variables into fuzzy or linguistic variables. In our case, we have two input variables: slope E and the variation of the slope CE. For more precise results we have designated seven, instead of five, intervals of the input variables called: large negative (NB), medium negative (NM), small negative (NS), zero (ZE), small positive (PS), medium positive (PM) and large positive (PB) [23]–[26]. Figures 6 and 7 show the membership functions of the input variables fuzzy subsets deduced from Tables 4 and 5.

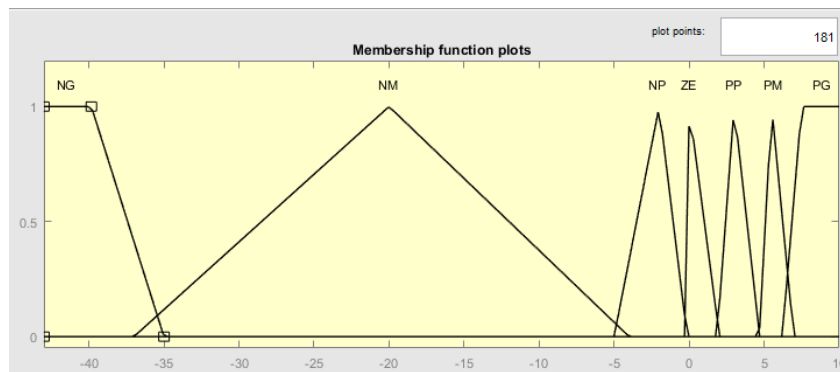


Figure 6. Membership function of input variables E

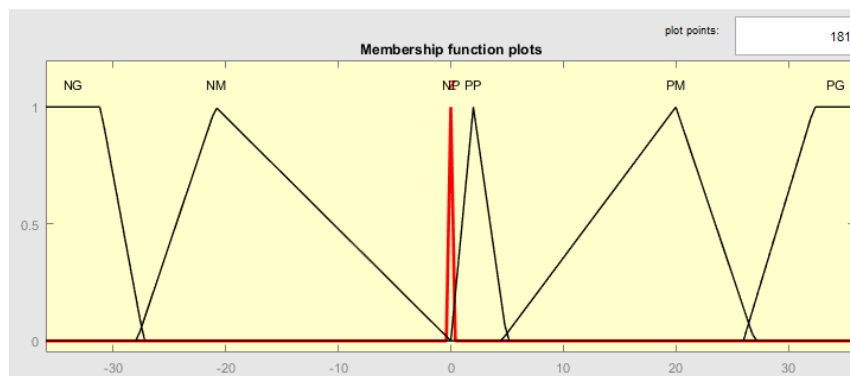


Figure 7. Membership function of input variables CE

**3.4. Inference and defuzzification**

Inference is the decision stage because we establish logical relationships between inputs and outputs while determining the rules of inference. Figure 8 defines the membership function of the output variable D. A thorough understanding of the system is essential for developing such a controller. Specifically, the input value is represented by two fuzzy functions with different degrees, and the output is defined by several functions. Several methods can fulfill this task.

We have chosen the Mamdani method for fuzzy inference, using MAX-MIN operations, where the MIN operator is applied for AND the MAX operator for OR. Based on these rules, an inference table can be drawn up as presented in Table 6. Finally, it is necessary to carry out the inverse operation of fuzzification and calculate a numerical value understandable by the external environment from a fuzzy definition. This process is known as defuzzification. The table of inference rules obtained from the behavioral study is asymmetrical, in contrast to the one derived from the  $p=f(v)$  curve, which is symmetrical. The simulation results of these two methods will be presented in the next section for comparison.

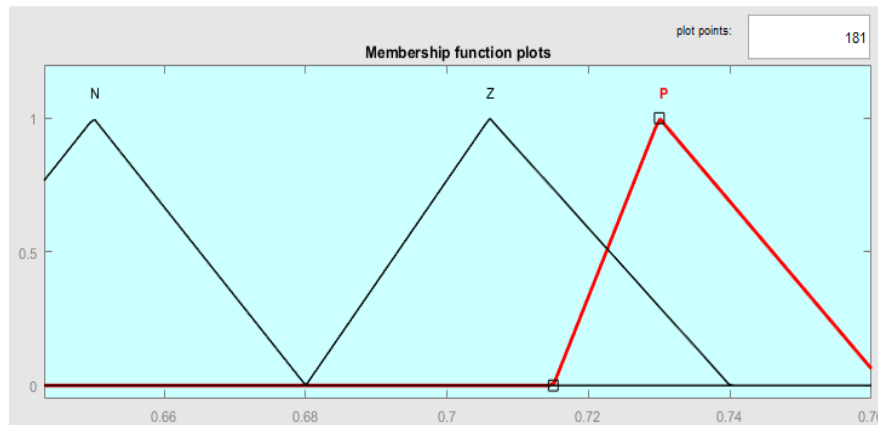


Figure 8. Membership function of output variables D

Table 6. Inference table for Asymmetrical FLC

CE \ E	PB	PM	PS	ZE	NS	NM	NB
PB	P	P	P	P	P	P	P
PM	Z	N	Z	Z	Z	P	Z
PS	N	Z	N	N	N	N	P
ZE	Z	N	Z	P	N	P	P
NS	Z	Z	P	P	P	P	Z
NM	P	P	P	P	P	P	P
NB	P	P	P	P	P	P	P

**4. SIMULATION AND RESULT**

**4.1. Simulation environment**

The complete architecture of the simulated system is shown in Figure 9, which provides an overview of the interconnection between the main functional blocks. To evaluate the performance of MPPT algorithms based on symmetrical and asymmetrical fuzzy logic, a series of numerical simulations was carried out using the MATLAB/Simulink environment. The simulated system includes a photovoltaic panel connected to a DC/DC converter Boost, controlled by an MPPT controller implemented using a fuzzy logic system.

**4.2. Simulation results under varying conditions**

The performance of the MPPT algorithms was evaluated by analyzing their response in terms of maximum power point (MPP) tracking time and overall system power efficiency. The simulations considered variations in environmental parameters, such as temperature and irradiance. Initially, the system was tested at a constant irradiance of 1000 W/m<sup>2</sup> while the temperature ranged from 55 °C down to 5 °C. The evolution of the output power for both the symmetrical and asymmetrical fuzzy logic controllers is illustrated in Figure 10.

We can clearly see that the output power based on asymmetrical FLC is greater than that of symmetrical FLC, the latter presenting anomalies in terms of stability, especially at high temperatures. Additionally, we carried out simulations at a temperature of 25 °C, with luminosity varying from 1000 W/m<sup>2</sup> to 500 W/m<sup>2</sup>, as shown in Figure 11. The output power evolutions of the two systems, based on the FLC symmetrical and the FLC asymmetrical methods, are presented in Figure 12. The power behavior at a temperature of 25 °C, with irradiance changing every 200ms from 1000 W/m<sup>2</sup> to 500 W/m<sup>2</sup>. The output power generated by symmetrical FLC is lower than that generated by asymmetrical FLC, especially in the luminosity range from 700 W/m<sup>2</sup> to 500w/m<sup>2</sup> at steady state. The performance of the system using asymmetrical fuzzy logic is incomplete in terms of power, which highlights the superiority of the asymmetrical FLC method in terms of output power and stability, especially in low-light conditions, as shown in Table 7.

It is important to note that the asymmetric FLC system improves the efficiency level of the system, especially at high temperatures and low luminosities [26]. The asymmetrical mode generates higher and more stable output powers than the symmetric mode in different conditions (climate of temperature and luminosity). However, the asymmetrical mode is more suitable for use in warmer regions and areas with low light.

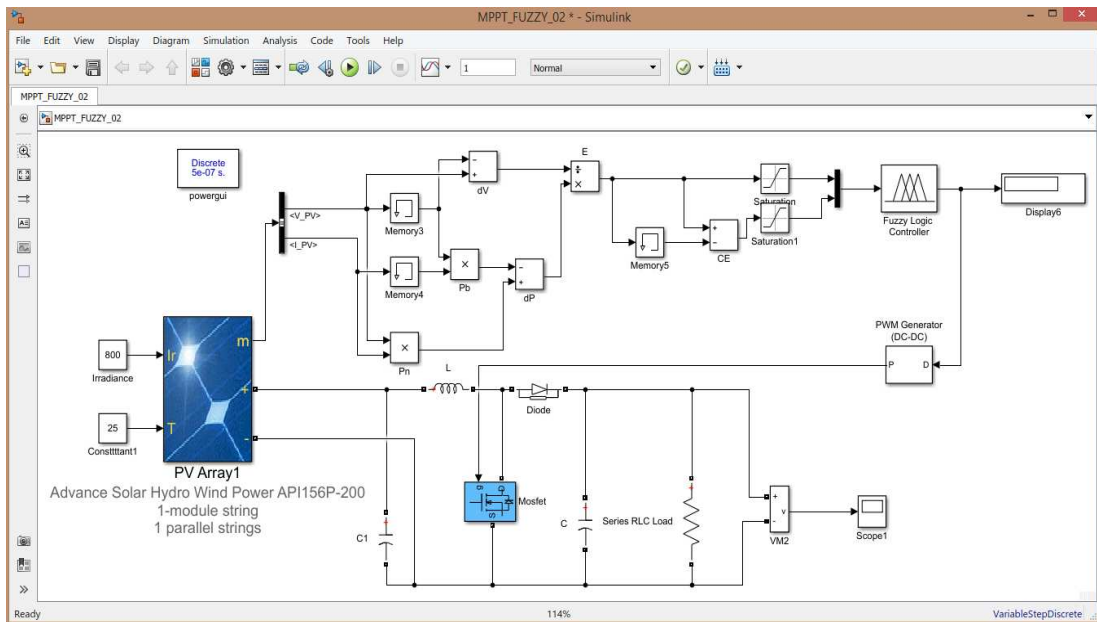


Figure 9. Architecture of the simulated PV system and fuzzy logic MPPT control scheme

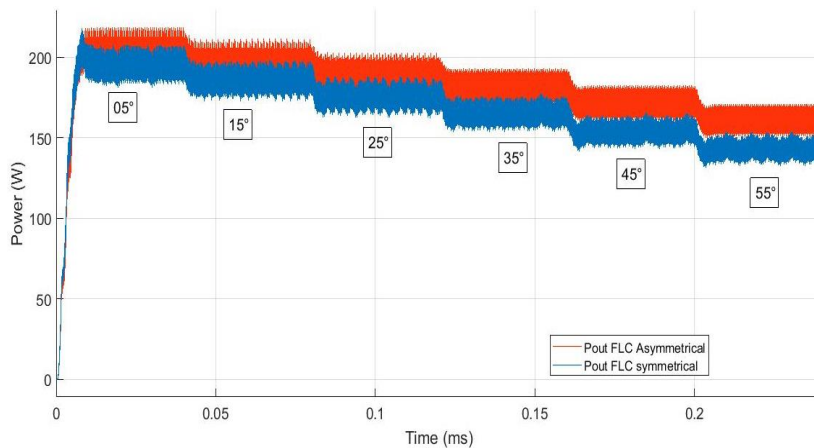


Figure 10. Output power with a decrease in temperature for Symmetrical FLC and Asymmetrical FLC

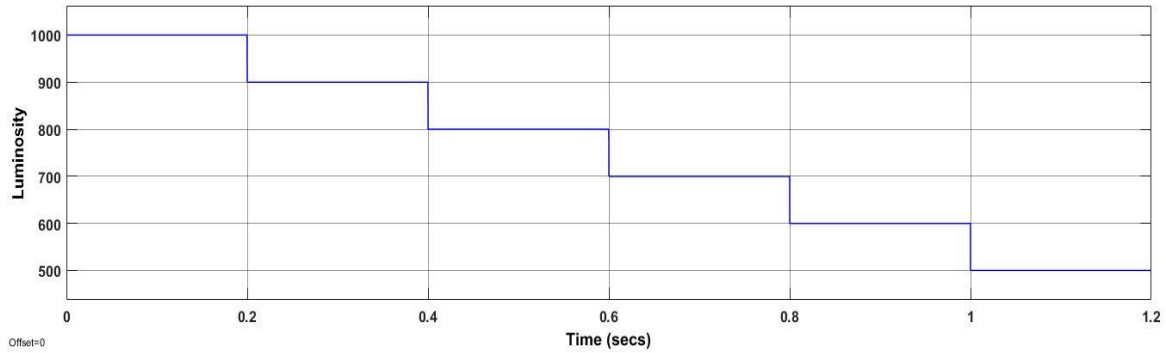


Figure 11. Change of luminosity at 25 °C

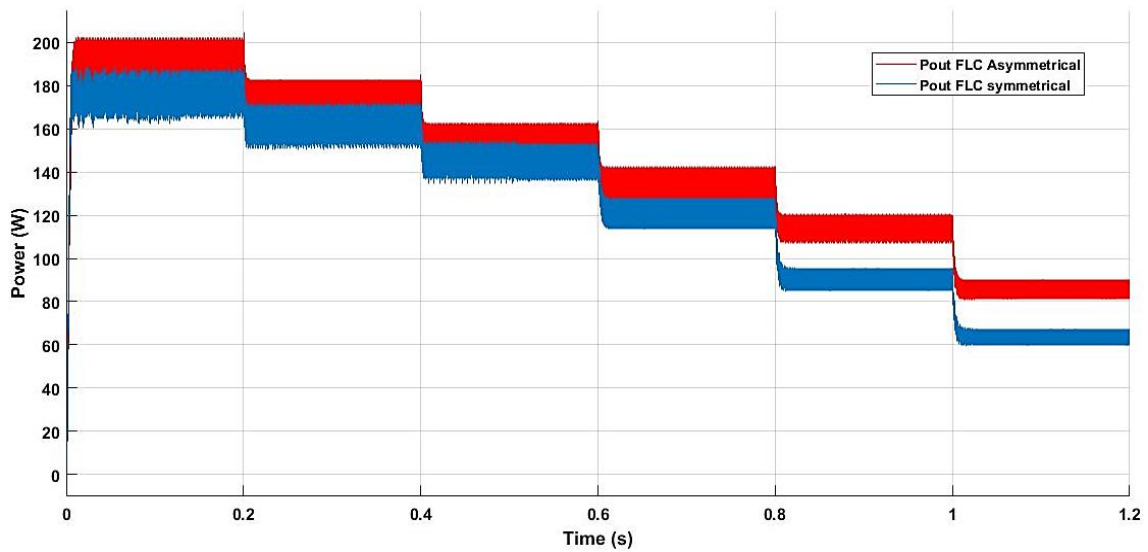


Figure 12. Output power with a decrease of luminosity for symmetrical FLC and asymmetrical FLC

Table 7. Shows the average power and efficiency of each method under different climatic conditions

Luminosity	Temperature	Pmax	Pout FLC Asymmetrical	Efficiency Asymmetrical	Pout FLC Symmetrical	Efficiency Symmetrical
1000	5	216	205	94.91%	195.3	90.42%
1000	15	207	197.1	95.22%	185.9	89.81%
1000	25	199.2	189.5	95.13%	176	88.35%
1000	35	190.9	182	95.34%	165.5	86.69%
1000	45	180.6	171.5	94.96%	154	85.27%
1000	55	169.2	161	95.15%	142.7	84.34%
900	25	180.3	171.9	95.34%	161.6	89.63%
800	25	161.2	153.6	95.29%	145.5	90.26%
700	25	141.3	134.5	95.19%	120.8	85.49%
600	25	119.8	114.2	95.33%	90.4	75.46%
500	25	92.3	86.8	94.04%	63.65	68.96%

### 5. CONCLUSION

In order to determine the input and output speech universe of the fuzzy logic-based controller, we carried out a study of the dynamic behavior of the PV system. This allowed us to extract the data from the stand-alone PV panel and define the membership functions for the maximum power point tracking controller algorithm. We compared the results of the Symmetric inference table, derived from the PV power versus voltage characteristic curve, with those of the asymmetric inference table, obtained from the PV behavioral study. This comparison led us to conclude that the asymmetric FLC method is more reliable in terms of power efficiency and stability (95%) under adverse conditions, such as high temperatures, low light, and shading.

## REFERENCES

- [1] Soedibyo, B. Amri, and M. Ashari, "The comparative study of Buck-boost, Cuk, Sepic and Zeta converters for maximum power point tracking photovoltaic using P&O method," in *2015 2nd International Conference on Information Technology, Computer, and Electrical Engineering (ICITACEE)*, IEEE, Oct. 2015, pp. 327–332. doi: 10.1109/ICITACEE.2015.7437823.
- [2] N. Karami, N. Moubayed, and R. Outbib, "General review and classification of different MPPT techniques," *Renewable and Sustainable Energy Reviews*, vol. 68, pp. 1–18, Feb. 2017, doi: 10.1016/j.rser.2016.09.132.
- [3] M. Kermadi and E. M. Berkouk, "Artificial intelligence-based maximum power point tracking controllers for Photovoltaic systems: comparative study," *Renewable and Sustainable Energy Reviews*, vol. 69, pp. 369–386, Mar. 2017, doi: 10.1016/j.rser.2016.11.125.
- [4] M. Zangeneh, E. Aghajari, and M. Forouzanfar, "A survey: fuzzify parameters and membership function in electrical applications," *International Journal of Dynamics and Control*, vol. 8, no. 3, pp. 1040–1051, Sep. 2020, doi: 10.1007/s40435-020-00622-1.
- [5] A. El-Rayyes and M. R. Elmorsy, "New 3-aryl-2-cyano-acrylohydrazide compounds as effective sensitizers for dye-sensitized solar cells: photovoltaic performance over the standard dye N719 upon co-sensitization," *Optical Materials*, vol. 132, p. 112866, Oct. 2022, doi: 10.1016/j.optmat.2022.112866.
- [6] S. Davoodabadi Farahani, B. Kazemi Majd, and A. M. Abed, "Control of thermal and fluid flow characteristics of an oscillating cylinder by porous media," *Alexandria Engineering Journal*, vol. 65, pp. 951–961, Feb. 2023, doi: 10.1016/j.aej.2022.10.003.
- [7] M. Hemmat Esfe and D. Toghraie, "Numerical investigation of wind velocity effects on evaporation rate of passive single-slope solar stills in Khuzestan province in Iran," *Alexandria Engineering Journal*, vol. 62, pp. 145–156, Jan. 2023, doi: 10.1016/j.aej.2022.07.015.
- [8] N. Hashim, Z. Salam, D. Johari, and N. F. Nik Ismail, "DC-DC boost converter design for fast and accurate MPPT algorithms in stand-alone photovoltaic system," *International Journal of Power Electronics and Drive Systems (IJPEDS)*, vol. 9, no. 3, p. 1038, Sep. 2018, doi: 10.11591/ijped.v9.i3.pp1038-1050.
- [9] A. El-Leathay, A. Nedelcu, S. Nicolaie, and R. A. Chihai, "Labview design and simulation of a small scale microgrid," *Series C: Electrical Engineering*, vol. 78, no. 1, pp. 235–246, 2016.
- [10] I. V. Banu, M. Istrate, D. Machidon, and R. Pantelimon, "Study regarding modeling photovoltaic arrays using test data in MATLAB/Simulink," *University Politehnica of Bucharest Scientific Bulletin Series C-Electrical Engineering and Computer Science*, vol. 77, no. 2, pp. 227–234, 2015.
- [11] S. M. Belhadj, B. Meliani, H. Benbouhenni, I. Colak, Z. M. S. Elbarbary, and S. F. Al-Gahtani, "Control of three-level quadratic DC-DC boost converters for energy systems using various technique-based MPPT methods," *Scientific Reports*, vol. 15, no. 1, p. 14631, Apr. 2025, doi: 10.1038/s41598-025-99551-2.
- [12] S. Mir *et al.*, "Effects of curvature existence, adding of nanoparticles and changing the circular minichannel shape on behavior of two-phase laminar mixed convection of Ag/water nanofluid," *Alexandria Engineering Journal*, vol. 66, pp. 707–730, Mar. 2023, doi: 10.1016/j.aej.2022.10.059.
- [13] O. Diouri, N. Es-Sbai, F. Errahimi, A. Gaga, and C. Alaoui, "Modeling and design of single-phase PV inverter with MPPT algorithm applied to the boost converter using back-stepping control in stand-alone mode," *International Journal of Photoenergy*, vol. 2019, pp. 1–16, Nov. 2019, doi: 10.1155/2019/7021578.
- [14] R. Ayop and C. W. Tan, "Design of boost converter based on maximum power point resistance for photovoltaic applications," *Solar Energy*, vol. 160, pp. 322–335, Jan. 2018, doi: 10.1016/j.solener.2017.12.016.
- [15] A. Pradhan and B. Panda, "A simplified design and modeling of boost converter for photovoltaic system," *International Journal of Electrical and Computer Engineering (IJECE)*, vol. 8, no. 1, p. 141, Feb. 2018, doi: 10.11591/ijece.v8i1.pp141-149.
- [16] M. A. Soliman, H. M. Hasanien, H. Z. Azazi, E. E. El-Kholy, and S. A. Mahmoud, "An adaptive fuzzy logic control strategy for performance enhancement of a grid-connected PMSG-based wind turbine," *IEEE Transactions on Industrial Informatics*, vol. 15, no. 6, pp. 3163–3173, Jun. 2019, doi: 10.1109/TII.2018.2875922.
- [17] C.-L. Liu, J.-H. Chen, Y.-H. Liu, and Z.-Z. Yang, "An asymmetrical fuzzy-logic-control-based MPPT algorithm for photovoltaic systems," *Energies*, vol. 7, no. 4, pp. 2177–2193, Apr. 2014, doi: 10.3390/en7042177.
- [18] C. B. N. Fapi, P. Wira, M. Kamta, and B. Colicchio, "Design and hardware realization of an asymmetrical fuzzy logic-based MPPT control for photovoltaic applications," in *IECON 2021 – 47th Annual Conference of the IEEE Industrial Electronics Society*, IEEE, Oct. 2021, pp. 1–6. doi: 10.1109/IECON48115.2021.9589287.
- [19] S. S. Kumar and K. Balakrishna, "A novel design and analysis of hybrid fuzzy logic MPPT controller for solar PV system under partial shading conditions," *Scientific Reports*, vol. 14, no. 1, p. 10256, May 2024, doi: 10.1038/s41598-024-60870-5.
- [20] S. Losada, D. F. Murcia, and S. O. García, "Design and implementation of a photovoltaic solar tracker using fuzzy control for SurColombiana," *ARNP J Eng Appl Sci*, vol. 12, no. 7, p. 6, 2017.
- [21] Y. Ravindranath Tagore, K. Rajani, and K. Anuradha, "Dynamic analysis of solar powered two-stage dc-dc converter with MPPT and voltage regulation," *International Journal of Dynamics and Control*, vol. 10, no. 6, pp. 1745–1759, Dec. 2022, doi: 10.1007/s40435-022-00930-8.
- [22] B. A. Amine, "Contribution to the improvement of maximum power point tracking control and optimization of the controller of an autonomous photovoltaic system," (in France) IbnTofail University, 2023.
- [23] S. Alam, S. Sulisty, I. W. Mustika, and R. Adrian, "Fuzzy adaptive hysteresis of RSS for handover decision in V2V VANET," *International Journal of Communication Networks and Information Security (IJCNIS)*, vol. 12, no. 3, pp. 433–439, 2020.
- [24] M. Haddin, A. Marwanto, A. Suprajitno, and M. Ismail, "Fuzzy logic applications for data acquisition systems of practical measurement," *International Journal of Electrical and Computer Engineering (IJECE)*, vol. 10, no. 4, p. 3441, Aug. 2020, doi: 10.11591/ijece.v10i4.pp3441-3450.
- [25] S. M. Belhadj, B. Meliani, H. Benbouhenni, S. Zaidi, Z. M. S. Elbarbary, and M. M. Alammam, "Control of multi-level quadratic DC-DC boost converter for photovoltaic systems using type-2 fuzzy logic technique-based MPPT approaches," *Heliyon*, vol. 11, no. 3, p. e42181, Feb. 2025, doi: 10.1016/j.heliyon.2025.e42181.
- [26] S. R. P. Chitturi, E. Sharma, and W. Elmenreich, "Efficiency of photovoltaic systems in mountainous areas," in *2018 IEEE International Energy Conference (ENERGYCON)*, IEEE, Jun. 2018, pp. 1–6. doi: 10.1109/ENERGYCON.2018.8398766.

**BIOGRAPHIES OF AUTHORS**

**Ahmed Amine Barakate**    received the Ph.D. degrees in electrical engineering and renewable energies at the Faculty of Sciences, Ibn Tofail University of Kenitra, Morocco in 2023. Administrator since 2011 (Head of the Logistics and Heritage Department) at the Ibn Tofail Faculty of Economics and Management of Kenitra. Graduated from master's degree in microelectronics, and was awarded by the Faculty of Sciences, Ibn Tofail, Kenitra in 2009. He can be contacted at email: [ahmedamine.barakate1@uit.ac.ma](mailto:ahmedamine.barakate1@uit.ac.ma).



**Sami Choubane**    graduated from master's degree in microelectronics, awarded by the Faculty of Sciences, Ibn Tofail, Kenitra in 2009. he has during his professional career ensured several positions of responsibility, notably in companies such as CIM and TECHNIPRO, both located in his hometown Mohammedia, he occupies at present the position of technical-commercial manager at BOM Africa, also and since 2021. He can be contacted at email: [c.sami206@gmail.com](mailto:c.sami206@gmail.com).



**Abdelkader Hadjoudja**    was an engineer and was awarded a doctorate in Microelectronic by the National Polytechnic Institute of Grenoble, France, in 1997. He worked for 6 years as PLD leader engineer software in Atmel, Grenoble, France, and as a consultant within design and reuse. Since July 2010, he became a full Professor of Electronics in Ibn Tofail University Kenitra. He can be contacted at email: [abdelkader.hadjoudja@uit.ac.ma](mailto:abdelkader.hadjoudja@uit.ac.ma).